THE JOURNAL OF PHYSICAL CHEMISTRY B

Article

pubs.acs.org/JPCB

Calorimetric Behavior of Phosphatidylcholine/Phosphatidylethanolamine Bilayers is Compatible with the Superlattice Model

Kwan Hon Cheng,*[,†,‡] Jorma Virtanen,[§] and Pentti Somerharju[⊥]

[†]Department of Physics and Astronomy, Trinity University, San Antonio, Texas 78212, United States

[‡]Department of Physics, Texas Tech University, Lubbock, Texas 79409, United States

[§]Nano Science Center, Department of Chemistry, University of Jyväskylä, Jyväskylä, Finland

[⊥]Institute of Biomedicine, Department of Biochemistry and Developmental Biology, University of Helsinki, Helsinki, Finland

Supporting Information

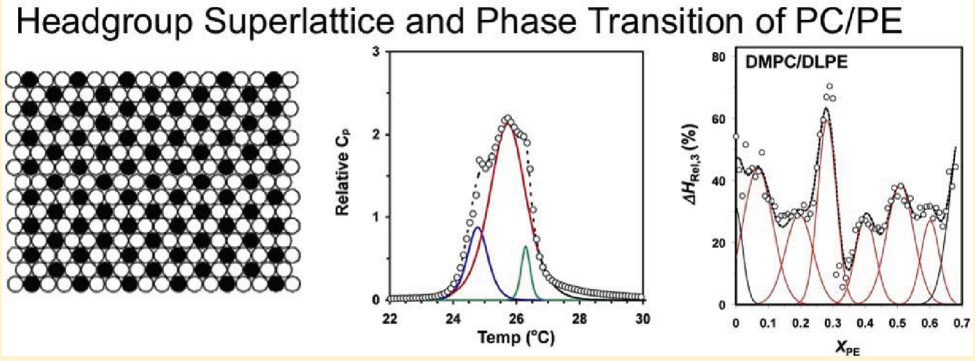

ABSTRACT: Differential scanning calorimetry was used to study the phase behavior of binary lipid bilayers consisting of phosphatidylcholine (PC) and phosphatidylethanolamine (PE) of varying acyl chain length. A two-state transition model was used to resolve the individual transition components, and the two-state transition enthalpy, the relative enthalpy, and the transition temperature of each component were plotted as a function of composition. Intriguingly, abrupt changes in these thermodynamic parameters were observed at or close to many "critical" X_{PE} values predicted by the *superlattice model* proposing that phospholipids with different headgroups tend to adopt regular rather than random lateral distributions. Statistical analysis indicated that the agreement between the observed and predicted "critical" compositions is highly significant. Accordingly, these data provide strong evidence that the molecules in PC/PE bilayers tend to adopt regular, superlattice-like lateral arrangements, which could be involved in the regulation of the lipid compositions of biological membranes.

1. INTRODUCTION

Lateral distribution of the lipids in biological membranes is an active field of study due to its functional implications in many key cellular processes. However, it is very difficult to obtain reliable data on biological membranes due to their highly complex composition. Therefore, many investigators have chosen to study model membranes consisting of only a limited number of lipid species. Apart from the popular raft-model proposing the presence of nanoscopic domains enriched in sphingolipids and cholesterol in cellular membranes,[1] we and others have proposed that different lipids tend to adopt regular, superlattice (SL)-like lateral distributions in fluid bilayers and cellular membranes as well.[2−4] It is important to note that such regular arrangements should not be considered as permanent or rigid (as implied by drawn models), but rather similar to *smectic A′*-phases, which are highly dynamic and lack long-range order.[5] Presumably, the tendency to adopt regular, SL-like distributions is mainly driven by repulsive steric or electrostatic interactions among similar molecules.[2] Intriguingly, the "critical" compositions predicted by the SL model could play a crucial role in the lipid homeostasis of cellular membranes by providing "set-points" regulating homeostatic phospholipases and synthetic enzymes as well.[6]

Evidence for SL-like distributions in phosphatidylcholine/phosphatidylethanolamine (PC/PE) bilayers has been obtained previously by using fluorescence and Fourier transform infrared (FTIR) spectroscopy.[7−10] In the present study, we used differential scanning calorimetry (DSC) to study the lateral organization of the components in several PC/PE bilayers. Although several DSC studies have been carried out with PC/PE mixtures previously,[11−15] the data point density in these studies was low, and thus largely precluded the

Received: August 15, 2011
Revised: December 11, 2011
Published: January 17, 2012

judgment of the presence of "critical" compositions indicative of SL formation. Accordingly, we varied the composition in very small increments (typically 1 mol %) and then plotted the transition temperature, relative enthalpy, and two-state transition enthalpy of the resolved transition peaks versus PE mole fraction. Intriguingly, we observed many of the critical compositions predicted by the SL model in a single PC/PE system, and virtually all of them in the four different PC/PE systems combined.

2. MATERIALS AND METHODS

2.1. Materials. The 1,2-dimyristoyl-*sn*-glycero-3-PC (DMPC), 1,2-dipalmitoyl-*sn*-glycero-3-PC (DPPC), 1,2-distearoyl-*sn*-glycero-3-PC (DSPC), 1,2-dilauroyl-*sn*-glycero-3-PE (DLPE), 1,2-dimyristoyl-*sn*-glycero-3-PE (DMPE), 1,2-dipalmitoyl-*sn*-glycero-3-PE (DPPE), 1,2-distearoyl-*sn*-glycero-3-PE (DSPE) and 1,2-dielaidoyl-*sn*-glycero-3-PE (DEPE) species were obtained from Avanti Polar Lipids (Alabaster, Alabama) and were free of impurities as analyzed by thin-layer chromatography. The solvents (LC-grade) were obtained from Merck and the other chemicals from Sigma.

2.2. Preparation of Multilamellar Liposomes. Calculated amounts of PC and PE dissolved in chloroform/methanol (9:1, v/v) were pipetted with extra care to a glass tube using Hamilton precision syringes equipped with a Cheney adapter. The syringe was chosen based on the volume to be pipetted in order to obtain the accuracy of ±1% specified by the pipet manufacturer. This accuracy can also be obtained in practice as tested in our previous studies using mass-spectrometry and deuterium-labeled internal standards.[16] After evaporation of the solvent under a nitrogen stream at 35−40 °C, the lipids were then dissolved in 0.5 mL of chloroform, and the solvent was again removed under a nitrogen steam at 60 °C. This protocol was used to prevent precipitation of PE before complete evaporation of the solvent, which can occur if methanol is present (unpublished data) as found previously for PC/cholesterol mixtures.[17] After evaporation of chloroform, the tubes were placed in high vacuum for 6 h to remove any residual solvent. Then 0.5 mL of Tris (10 mM)−EDTA (1 mM)−NaCl (50 mM) buffer, pH 7.0, was added, and the tubes were kept in a 70 °C water bath for 1 min, vortexed, and moved to an ice−water bath for 3 min. This heating−cooling cycle was repeated 5 times, and the samples were subsequently stored at 4 °C in the dark.

2.3. DSC Measurements. A high-sensitivity 6100 Nano II DSC instrument from Calorimetric Sciences (Lindon, Utah) was used to obtain sequential heating and cooling scans (0.5 °C/min) of samples containing 1 μmol of phospholipid. The scans were repeated for several samples in each set with essentially identical results. A limited set of samples was also analyzed using a heating rate of 0.05 °C/min.

2.4. The Multiple Two-State Transition Model. A DSC apparatus measures the specific heat capacity $C_p(T)$ as a function of temperature T, i.e., the temperature derivative of the total excess molar heat capacity $h(T)$ versus T.[18] The multiple two-state transition model assumes that the system has n independent transitions and that each of these multiple transitions is characterized by a separate and unique transition temperature (T_i) and an excess molar heat capacity $h_i(T)$. If $\alpha_i(T)$ denotes the fraction of molecules of the ith component that has completed the transition at the temperature T, the multiple two-state transition model provides a relationship between $h_i(T)$ and $\alpha_i(T)$:

$$c_p(T) = \frac{d}{dT}h(T) = \frac{d}{dT}\left[\sum_{i=1}^{n} h_i(T)\right] = \left[\sum_{i=1}^{n} \frac{d}{dT}[\alpha_i(T)]\cdot\Delta H_i\right] \quad (1)$$

where

$$\alpha_i(T) = \frac{\exp\left[-\frac{\Delta H_{2S,i}}{RT}\left(1-\frac{T}{T_i}\right)\right]}{1+\exp\left[-\frac{\Delta H_{2S,i}}{RT}\left(1-\frac{T}{T_i}\right)\right]} \quad (2)$$

Here R is the gas constant, $\Delta H_{2S,i}$ is the two-state transition enthalpy, and ΔH_i is the enthalpy of the ith independent component. For each ith component, the multiple two-state transiton model predicts that all molecules in a cooperative unit undergo the phase transition simultaneously, and thus $\Delta H_{2S,i}$ represents the collective enthalpy of one cooperative unit. The number of molecules in a cooperative unit ($N_{c,i}$) can be estimated by dividing $\Delta H_{2S,i}$ by ΔH_i (eq 3).

$$N_{c,i} = \frac{\Delta H_{2S,i}}{\Delta H_i} \quad (3)$$

The values of T_i, $\Delta H_{2S,i}$, and ΔH_i for each resolved component were obtained by fitting eq 1 to DSC data using nonlinear regression. Figure 1S in the Supporting Information demonstrates the dependence of $\alpha_i(T)$, $C_p(T)$, and $N_{c,i}$ on $\Delta H_{2S,i}$ using simulation. Since the absolute value of ΔH_i depends on the quantity of lipid in the sample cell, which may vary slightly, we used a relative value $\Delta H_{Rel,i}$ as defined by eq 4:

$$\Delta H_{Rel,i} = \frac{\Delta H_i}{\sum_{i=1}^{n}\Delta H_i} \quad (4)$$

The χ^2 value indicating the goodness of fit was determined from eq 5:

$$\chi^2 = \sum_{i=1}^{N}(y_i - y_i^p)^2\cdot\Delta T \quad (5)$$

where y_i and y_i^p are the ith experimental and predicted data points, respectively, while N is the total number of data points, and ΔT is the temperature increment.

2.5. Deconvolution of Resolved Thermodynamic Parameters versus Composition Plots. A multiple Gaussian-option of the PeakFit software (Jandel Scientific, San Rafael, CA) was employed to deconvolute the resolved $\Delta H_{2S,i}$ or $\Delta H_{Rel,i}$ according to the multiple two-state transition model versus X_{PE} plots. A high frequency filter was applied to assist in fitting so that peaks that are defined by less than three data points were not included in the peak search procedure.[8]

2.6. SL Model. According to the SL model, the guest molecule can adopt either a hexagonal (HX), centered rectangular (CR) or rectangular (R) distribution in a host lattice of a hexagonal symmetry, and the allowed (critical) compositions can be derived from simple geometrical principles.[2] For $X_{PE} < 0.5$ (i.e., when PE is the guest and PC the host), the critical X_{PE}'s

dx.doi.org/10.1021/jp2078488 | J. Phys. Chem. B 2012, 116, 1802−1811

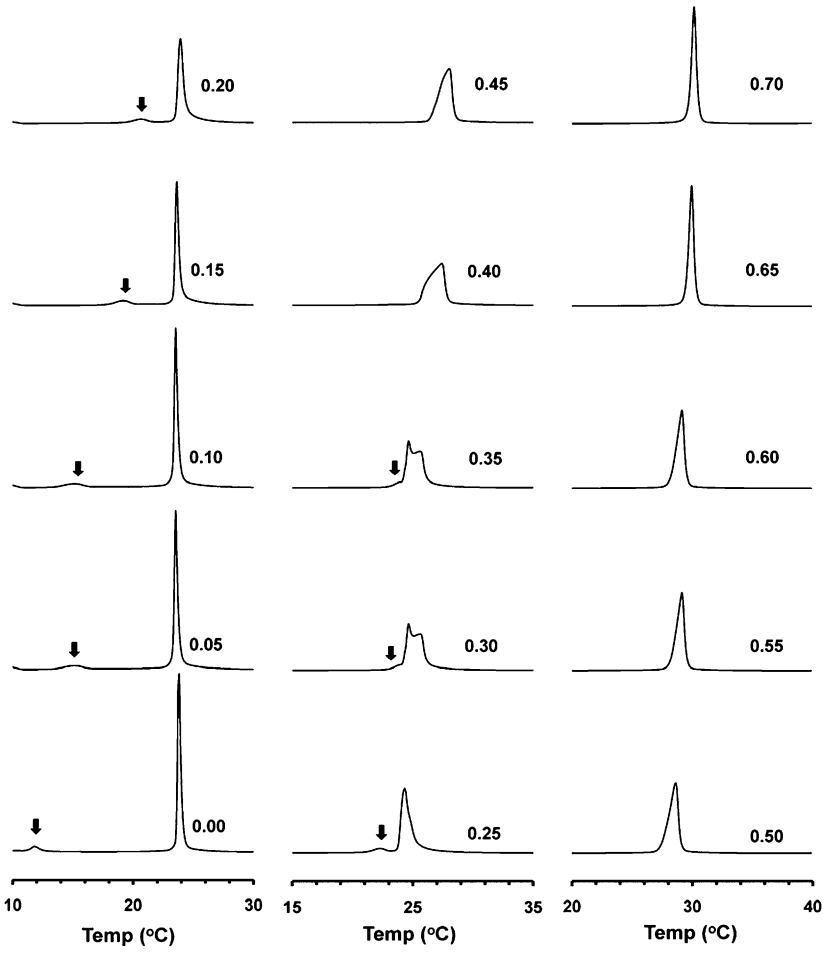

Figure 1. Representative DSC heating scans for DMPC/DLPE bilayers. The peak areas have been normalized to ease comparison. Arrowhead indicates the pretransition.

for superlattices with a HX, CR, or R symmetry are given by eqs 6−8:[10,19]

$$X^{HX} = 1/(a^2 + ab + b^2) \quad (6)$$

$$X^{CR} = 1/(2ab + b^2) \quad (7)$$

$$X^{R} = 1/(ab + b^2/2) \quad (8)$$

When $X_{PE} > 0.5$ (i.e., when PE is the host and PC is the guest), the critical X_{PE}'s are given by eqs 9−11:

$$X^{HX} = 1 - 1/(a^2 + ab + b^2) \quad (9)$$

$$X^{CR} = 1 - 1/(2ab + b^2) \quad (10)$$

$$X^{R} = 1 - 1/(ab + b^2/2) \quad (11)$$

where a and b indicate the distance in lattice sites between two proximal guest molecules along the principal host lattice axes.[3] If the guests form pairs (dimers), the values of the critical X_{PE}'s are twice those for monomeric guests (see Supporting Information).

3. RESULTS

3.1. Calorimetric Behavior of PC/PE Bilayers. DSC heating scans at a rate of 0.5 °C/min were recorded for bilayers consisting of DMPC/DLPE, DMPC/DMPE, DPPC/DMPC, DSPC/DMPE, and DSPC/DEPE with X_{PE} varying in 1 mol % increments. Representative scans for DMPC/DLPE bilayers are presented in Figure 1. For neat DMPC (X_{PE} = 0), the peak temperature of the pre- (T_p) and main (T_m) transitions were found at 11.4 and 23.5 °C, respectively, in agreement with previous data.[20] When X_{PE} was gradually increased to 0.30, T_p increased steadily, whereas T_m remained relatively constant. The pretransition eventually disappeared or merged with the main transition at X_{PE} of 0.30−0.35, while the main transition became broader and eventually developed a pronounced shoulder. Above X_{PE} of 0.40, the main transition narrowed again so that its width at X_{PE} of 0.65 was similar to that at X_{PE} of 0.20. DSC scans for DMPC/DMPE bilayers are presented in Figures 2SA and 2SB in the Supporting Information. The difference between the T_m's of the PC and PE components in the DMPC/PMPE system is the largest among the PC/PE systems in this study. A similar behavior of merging of T_m/T_p and broadening of the main transition was also detected. No obvious phase separation was detected within the composition range reported in this study.

Additional cooling (0.5 °C/min) and "slow" heating (0.05 °C/min) scans were recorded for a limited number of samples of the different PC/PE mixtures. Figure S3 in the Supporting Information compares data for the heating, cooling, and slow scans of DMPC/DLPC bilayers with X_{PE} of 0.29−0.38. In general, the shapes, locations, and relative enthalpies of the transition components are very similar among the heating,

dx.doi.org/10.1021/jp2078488 | J. Phys. Chem. B 2012, 116, 1802−1811

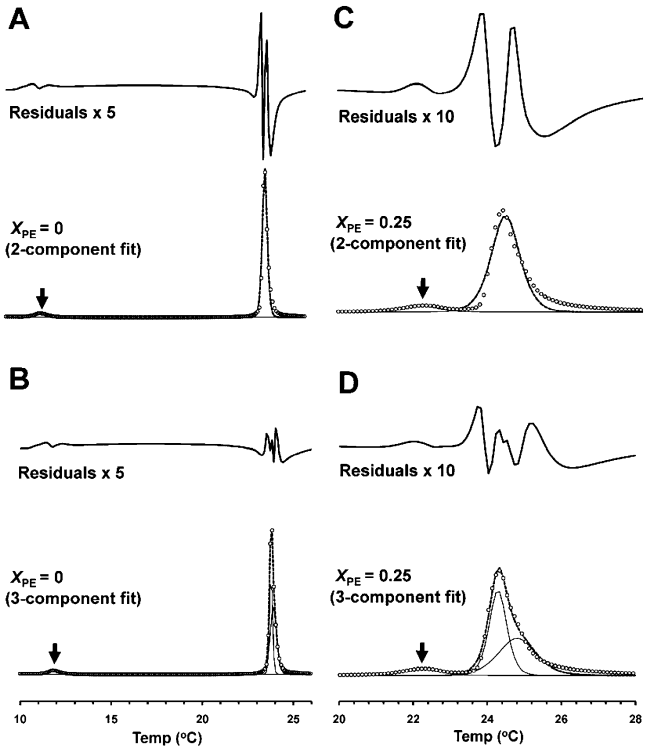

Figure 2. Multicomponent fits to DSC data for DMPC/DLPE bilayers in the presence of pretransition. X_{PE} is 0 (A,B) or 0.25 (C,D). Fits assuming two (A,C) or three (B,D) components are shown. Open circles represent the experimental data points, the solid line represents the fitted peaks, and the dotted line represents the sum of all fitted peaks. The pretransition is indicated by an arrowhead. Residuals are shown at the top of each panel.

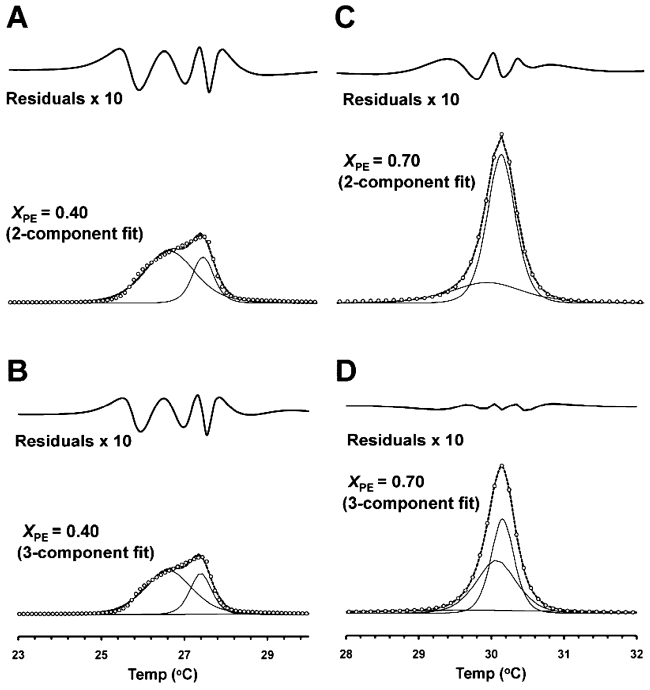

Figure 3. Multicomponent fits to the DSC data for DMPC/DLPE bilayers in the absence of pretransition. X_{PE} is 0.40 (A,B) or 0.70 (C,D). The two-state transition peaks based on fits assuming two (A,C) or three (B,D) components are shown. Fitting residuals are shown at the top of each panel.

cooling, and slower scans for the same X_{PE}. Notably, the lack of significant hysteresis between cooling and heating scans implies that the lateral organization of the bilayer is similar in the gel and liquid-crystalline states. The pretransition showed some hysteresis (e.g., for X_{PE} = 0.29 T_1 was ~20 °C in the cooling scan vs ~23 °C in the heating scan), which is most probably due to the slowness of this transition.[21,22]

Since the main phase transition of PC/PE bilayers was often asymmetric and in some cases exhibited more than one peak as demonstrated in Figure 1, a multiple two-state transition model (see Materials and Methods) was used to resolve the components. Figures 2 and 3 show examples of two- and three-component fits before (X_{PE} = 0 and 0.25) and after (X_{PE} = 0.40 and 0.70) the merge of the pre- and main transitions, while Table 1 summarizes the goodness of fit (χ^2) values and the parameters T_i, $\Delta H_{2S,i}$, and $\Delta H_{Rel,i}$. When the pretransition was detectable ($0 < X_{PE} < 0.3$), much better fits were obtained by assuming three rather than two components in total (Figure 2). In the absence of the (visible) pretransition (i.e., $X_{PE} > 0.3$), the three-component model generally did not improve the fit as compared to the two-component model (Figure 3), except in a few cases (e.g., χ^2 of 0.004 versus 0.014 for X_{PE} = 0.70) as shown in Table 1. This improvement, however, is most probably an artifact due to the fact that the fitting protocol erroneously indicated a curving baseline as a very broad transition. Accordingly, the presence of either two or three transitions overall were assumed in the absence or presence of the pretransition, respectively. For consistency, the parameters for the pretransition are referred to as T_1, $\Delta H_{2S,1}$ and $\Delta H_{Rel,1}$, while those for the first and second main transition components are referred to as T_2, $\Delta H_{2S,2}$, and $\Delta H_{Rel,2}$ and T_3, $\Delta H_{2S,3}$, and $\Delta H_{Rel,3}$, respectively.

The resolved transition temperatures T_1, T_2, and T_3 obtained from the multiple two-state transition fits are plotted as a function of X_{PE} for DMPC/DLPE bilayers in Figure 4A. The T_1 plot indicates that the pretransition is present up to X_{PE} of 0.38−0.40, thus marking this value as a critical one. Other critical compositions are indicated by kinks at X_{PE} of ~0.13, 0.21, and 0.32. The pretransition was abolished or became undetectable at X_{PE} of ~0.20 for both DMPC/DMPE and DPPC/DMPE and ~0.25 for DSP/DMPE (Figure 4B−D) thus marking these compositions as critical ones as well. Interestingly, the χ^2 values of two- and three-component fits showed local minima and merger of the two- and three-component fits at or close to predicted critical compositions (see Figure S4 of the Supporting Information).

3.2. Relative Enthalpy versus Composition Plots.

Figures 5 and 6 show the relative enthalpies of the resolved pretransition (i = 1) and the second main transition (i = 3) components, i.e., $\Delta H_{Rel,1}$ and $\Delta H_{Rel,3}$, respectively, versus X_{PE} for the different mixtures of saturated PC and PE. As $\Delta H_{Rel,2}$ = 100 − $\Delta H_{Rel,1}$ − $\Delta H_{Rel,3}$, plots of $\Delta H_{Rel,2}$ are redundant and thus not shown. Since the resolved thermodynamic parameter versus X_{PE} plots indicated the presence of multiple overlapping peaks, Gaussian deconvolution was carried out. Among the resolved peaks, only those (indicated by a red line) defined by more than two data points and of a reasonable width were considered relevant, while those (indicated by a black line) defined by one or two data points or were unreasonably broad were rejected. The rejection of a broad deconvoluted peak was based on the criterion of fwhm of the resolved Gaussian peak > X^*_{PE} ($1 - X^*_{PE}$), where fwhm denotes the full width half-maximum

dx.doi.org/10.1021/jp2078488 | J. Phys. Chem. B 2012, 116, 1802−1811

Table 1. Representative Resolved Thermodynamic Parameters (T_i, $\Delta H_{2s,i}$, $\Delta H_{Rel,i}$) of DMPC/DLPE Based on the Multi-Component Two-State Transition Models[a]

	two-component fit				three-component fit			
X_{PE}	T_i (°C)	$\Delta H_{2s,i}$ (kcal/mol)	$\Delta H_{Rel,i}$ (%)	χ^2	T_i (°C)	$\Delta H_{2s,i}$ (kcal/mol)	$\Delta H_{Rel,i}$ (%)	χ^2
0	11.83	548	7.95	0.67	11.80	548	7.61	0.10
	23.79	2075	92.05		23.75	3615	38.20	
					23.97	1538	54.19	
0.25	22.14	604	8.16	0.43	22.17	518	8.5	0.11
	24.37	717	91.84		24.26	1116	47.35	
					24.77	524	44.15	
0.40	26.61	462	72.80	0.04	26.58	476	68.16	0.04
	27.37	1100	27.20		27.36	1057	28.94	
					29.34	384	2.90	
0.70	29.91	592	26.41	0.014	29.65	189	12.37	0.004
	30.00	1515	73.59		30.25	1000	43.23	
					30.11	1742	44.39	

[a]The relative chisquare (χ^2) values of the fits are also shown.

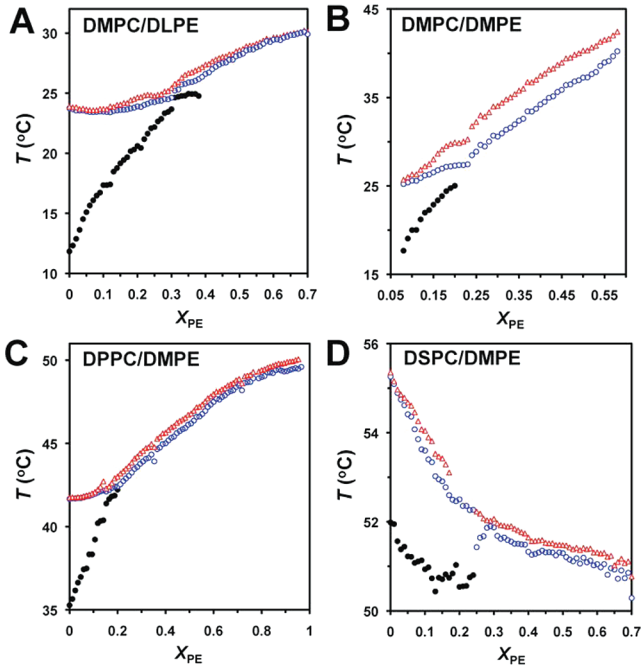

Figure 4. Peak transition temperatures vs X_{PE} for different PC/PE bilayers. (A) DMPC/DLPE, (B) DMPC/DMPE, (C) DPPC/DMPE, and (D) DSPC/DMPE. Temperature of the pretransition (filled black circles) and that of the two resolved main transition components (blue circles and red triangles) are shown.

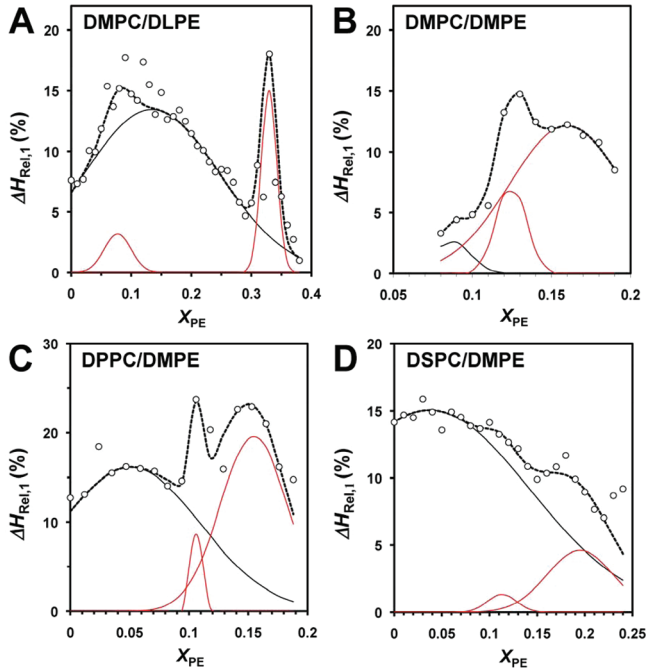

Figure 5. Relative enthalpy of the pretransition ($\Delta H_{Rel,1}$) versus X_{PE} for different PC/PE bilayers. (A) DMPC/DLPE, (B) DMPC/DMPE, (C) DPPC/DMPE, and (D) DSPC/DMPE. The data points are indicated by open circles, the deconvoluted Gaussian peaks are denoted by a red line, and their sum is represented by a dotted line. The Gaussians drawn in black were rejected because they did not fit the criteria of acceptance (see text).

and X^*_{PE} is the adjacent critical PE composition predicted by the SL model.[2] This "wide" peak rejection criterion, although somehow arbitrary, allowed us to take into account the general trend of the greater separation between consequent predicted critical compositions with increasing X_{PE}.

In the case of DMPC/DLPE bilayers, peaks at X_{PE} of ~0.08 and 0.33 were observed in the $\Delta H_{Rel,1}$ plot (Figure 5A) and at ~0.2, 0.28, 0.4, 0.51, and 0.6 in the $\Delta H_{Rel,3}$ plot (Figure 6A). Several peaks in the $\Delta H_{Rel,1}$ and $\Delta H_{Rel,3}$ plots were also observed for the other PC/PE mixtures (Figures 5 and 6) and are summarized in Table 2. Besides the saturated systems, we also studied the DSPC/DEPE bilayers in which the acyl chains of PE have trans-double bonds. No pretransition was observed for this system, and thus only the main transition was analyzed. The plot of the relative enthalpy $\Delta H_{Rel,3}$ showed peaks at X_{PE} of ~0.21 and 0.25 (Figure S5 in the Supporting Information).

3.3. Two-State Transition Enthalpy versus Composition Plots. To obtain additional evidence on the presence of critical compositions, we determined the two-state transition enthalpies ($\Delta H_{2S,i}$) of the resolved transitions and plotted them as a function of X_{PE}. $\Delta H_{2S,i}$ is a measure of the cooperativity of a phase transition (see Materials and Methods and Figure S1 of the Supporting Information). Figure 7 shows the two-state enthalpy ($\Delta H_{2S,1}$) of the pretransition versus X_{PE} for the different PC/PE mixtures. Clear peaks are observed in all mixtures except DPPC/DMPE. Some peaks are also observed in the $\Delta H_{2S,2}$ and

dx.doi.org/10.1021/jp2078488 | J. Phys. Chem. B 2012, 116, 1802–1811

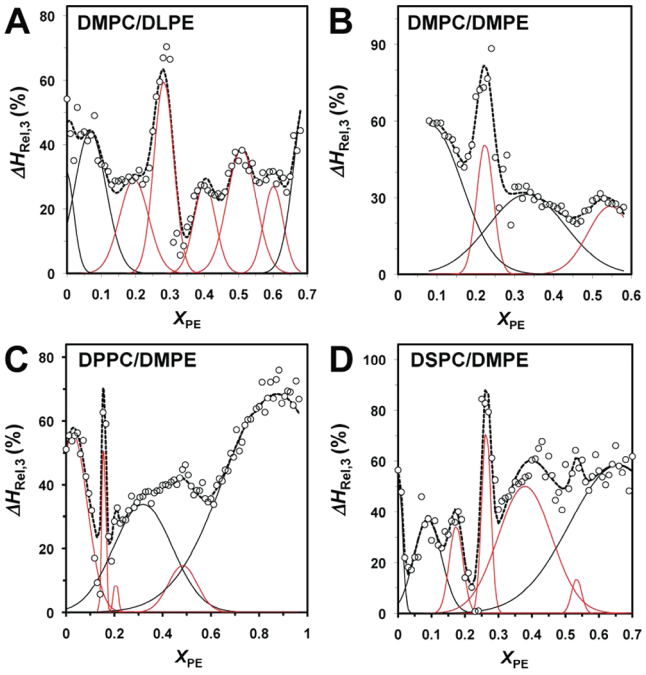

Figure 6. Relative enthalpy of the second resolved main transition component ($\Delta H_{Rel,3}$) versus X_{PE} for different PC/PE bilayers. (A) DMPC/DLPE, (B) DMPC/DMPE, (C) DPPC/DMPE, and (D) DSPC/DMPE. See the caption of Figure 5 for details.

$\Delta H_{2S,3}$ plots (Figures 8 and 9). For the DSPC/DEPE system, peaks at ~0.17, 0.27 and (possibly) at 0.37 were observed in the $\Delta H_{2S,3}$ versus X_{PE} plot (Figure S5 in the Supporting Information). The X_{PE} values of the indicated peaks are summarized in Table 2.

We also determined the size of the cooperative unit, i.e., $N_{C,i} = \Delta H_{2S,i}/\Delta H_i$ as a function of X_{PE} for DMPC/DLPC bilayers. Sharp and prominent peaks were observed at ~0.33, 0.28, and 0.33 for the pretransition and the two main transition components, respectively (Figure S6 in the Supporting Information). Probable negative peaks were observed at ~0.2, 0.3, 0.4, and 0.5. See Discussion for the relevance of such negagative peaks. All these compositions agree favorably with the critical compositions predicted by the SL model.[2]

3.4. Correlation between the Observed and the Predicted Critical Compositions. In order to quantitatively evaluate the significance of the data in Table 2, a rigorous statistical analysis using the binomial distribution model[23] was performed (see Supporting Information). The analysis included eight predicted critical points within the range of X_{PE} = 0.18–0.70, i.e., 0.200, 0.250, 0.286, 0.333, 0.400, 0.500, 0.600, and 0.667. Values below X_{PE} of 0.18 were excluded because the spacings between the predicted critical compositions are less that 2 mol % (twice the probable error of ~1 mol % in our sample composition) used in this study. The X_{PE} values above 0.677 were excluded because only a few samples were in that composition range.

As shown in Table 2, 47 critical compositions were observed experimentally at $0.18 < X_{PE} < 0.7$. Among these, 27 compositions deviated by less than 1 mol % and 33 compositions deviated by less than 2 mol % from the closest predicted critical composition. Statistical analysis based on the binomial distribution model[23] (see Supporting Information) showed that the probability that 27 observed critical values would lie within ±1 mol % of eight predicted ones *just by chance* is one out of 1.3×10^4. In other words, it is highly unlikely that so many experimentally observed values would lie so close to the predicted ones simply by chance. The concurrence of the experimental and predicted critical compositions is visualized in Figure S7 of the Supporting Information. Notably, this figure also shows that the observed critical compositions are more frequent and more closely spaced at low PE mole fractions, as predicted by the SL model.[2,10,19] In conclusion, these statistical analyses strongly support the notion that multiple, SL-like arrangements of the component lipids are sequentially formed in PE/PC bilayers when the composition is varied.

4. DISCUSSION

The present study shows that the calorimetric behavior of binary PC/PE bilayers is complex, i.e., multiple transition components are detected. Besides the pretransition, the main transition typically consists of two components (Figures 1 and 2). To account for this complex behavior, we employed a multiple two-state transition model assuming the presence of independent transition components defined by a unique set of thermodynamic parameters. Each *i*th component is characterized by the resolved transition temperature (T_i), relative enthalpy ($\Delta H_{Rel,i}$), and two-state transition enthalpy ($\Delta H_{2s,i}$). The multiple two-state transition model represents a convenient way to analyze complex systems such as PE/PC bilayers. While this model probably oversimplifies the situation by assuming that coexisting domains undergo the transition independently, models accounting for putative interdomain interactions are too complex to be implemented here.

Our results indicate that some or all of the resolved thermodynamic parameters change abruptly at particular compositions. Intriguingly, these compositions typically agree closely with critical compositions predicted by the SL model, proposing that the headgroup of the guest lipid tends to adopt regular lateral distribution with a rectangular, centered-rectangular or hexagonal symmetry in the host lipid lattice.[2,10,19] The SL model states that when the mole fraction of the guest increases, (i) multiple superlattices with increasing guest density are formed sequentially, and (ii) the bilayer area covered by a particular superlattice peaks at each critical composition.[2] Because lipid packing in superlattice domains is predicted and also indicated by molecular dynamics (MD) simulations[24] to be tighter than in domains of random organization, the transition enthalpy and cooperativity in the former are expected be higher than in the latter. As shown in Table 2, the observed maxima of $\Delta H_{2s,i}$ and/or $\Delta H_{Rel,i}$ nearly always coincide within 1–2 mol % with predicted critical compositions. Statistical analysis (see Supplementing Information) indicated that the probability for fortuitous agreement between so many observed and predicted critical compositions is very low. Accordingly, the present calorimetric data provides strong support for the idea that multiple different superlattices can be present in gel-state PC/PE bilayers.

Unlike the transition enthalpy, the size of the co-operative unit does not need to correlate with the mode of lateral organization (superlattice versus random). Tighter packing of the lipids in superlattice domains may reduce the bilayer curvature as compared to random domains of similar composition, thus increasing the size of the cooperative unit. Alternatively, tighter packing in superlattice domains could result in increased curvature, thus reducing the size of the cooperative unit as compared to random domains. Accordingly, depending on the ratio

dx.doi.org/10.1021/jp2078488 | J. Phys. Chem. B 2012, 116, 1802–1811

Table 2. Critical X_{PE}'s Based on Deviations (or Merger) of the T_p and T_m Plots and the Peaks (± Half Width) of the Two-State Transition Enthalpy ($\Delta H_{2S,1}$(p), $\Delta H_{2S,2}$(m), $\Delta H_{2S,3}$(m)) and Relative Enthalpy ($\Delta H_{Rel,1}$(p), $\Delta H_{Rel,3}$(m)) Plots Associated with the Pre- (p) and Main Transitions (m)[a]

$X_{PE}^{R,CR,HX}$	T_p/T_m	$\Delta H_{2S,1}$(p)	$\Delta H_{2S,2}$(m)	$\Delta H_{2S,3}$(m)	$\Delta H_{Rel,1}$(p)	$\Delta H_{Rel,3}$ (m)
$0-0.111^{R,CR,HX}$		0.084 ± 0.054^{1}	0.077 ± 0.065^{1}		0.077 ± 0.071^{1}	
$0.111^{CR,HX}$		0.111 ± 0.099^{2}			0.108 ± 0.009^{3}	
					0.113 ± 0.036^{4}	
$0.125^{CR,R}$		0.154 ± 0.030^{4}			0.125 ± 0.022^{2}*	
$0.143^{CR,HX}$						
0.167^{R}		0.172 ± 0.111^{1}	0.158 ± 0.016^{3}	0.178 ± 0.041^{2}	0.160 ± 0.085^{2}	0.159 ± 0.018^{3}
				0.174 ± 0.050^{3}	0.155 ± 0.067^{3}	0.173 ± 0.048^{4}
				0.172 ± 0.086^{5}		
0.200^{CR}	0.200^{2}*	0.215 ± 0.077^{4}	0.209 ± 0.043^{2}*	0.210 ± 0.029^{4}*	0.195 ± 0.082^{4}*	0.196 ± 0.100^{1}*
	0.200^{3}*		0.197 ± 0.082^{4}*			0.224 ± 0.051^{2}
						0.208 ± 0.022^{3}*
						0.214 ± 0.011^{5}
$0.250^{R,CR,HX}$	0.250^{4}*	0.254 ± 0.057^{1}*		0.257 ± 0.059^{1}*		0.264 ± 0.032^{4}
				0.265 ± 0.094^{2}		0.248 ± 0.062^{5}*
				0.257 ± 0.128^{3}*		
				0.266 ± 0.083^{5}		
†$0.286^{CR,HX}$		0.288 ± 0.029^{1}*	0.281 ± 0.053^{1}*			0.282 ± 0.068^{1}*
$0.333^{CR,\ HX}$		0.315 ± 0.008^{1}	0.312 ± 0.119^{2}	0.331 ± 0.053^{1}*	0.329 ± 0.030^{1}*	
			0.305 ± 0.050^{4}	0.326 ± 0.121^{4}*		
†0.400^{CR}	0.380^{1}	0.370 ± 0.068^{1}		0.408 ± 0.106^{1}*		0.401 ± 0.098^{1}*
				0.372 ± 0.152^{2}		0.379 ± 0.188^{4}
				0.396 ± 0.118^{3}*		
				0.427 ± 0.167^{4}		
				0.367 ± 0.229^{5}		
0.500^{R}				0.467 ± 0.055^{2}		0.509 ± 0.099^{1}*
				0.483 ± 0.041^{4}		0.489 ± 0.143^{3}*
						0.534 ± 0.035^{4}
						0.546 ± 0.137^{2}
†0.600^{CR}				0.599 ± 0.044^{3}*		0.601 ± 0.067^{1}*
$0.667^{CR,HX}$			0.689 ± 0.175^{1}			
			0.677 ± 0.036^{4}			
$0.857^{CR,HX}$				0.846 ± 0.064^{3}		
$0.875^{CR,R}$						

[a]Predicted critical X_{PE}'s from the SL model of rectangular (R), center-rectangular (CR), and hexagonal (HX) symmetry are shown. Superscripts 1−5 correspond to DMPC/DLPE, DMPC/DMPE, DPPC/DMPE, DSPC/DMPE, and DSPC/DEPE bilayers, respectively. The predicted critical X_{PE}'s that are separated by less than 0.01 in the range of $0.2 \leq X_{PE} < 0.7$ are indicated by superscript *. The observed critical X_{PE} that does not match the predicted X_{PE}'s within ±0.03 is in bold. The predicted critical X_{PE}'s of 0.286, 0.400, and 0.600 indicated by superscript † correspond to superlattices of dimeric guests, i.e., 2×0.143, 2×0.200 and $(1 - 2 \times 0.200)$, respectively. See Materials and Methods for details.

of the components in a particular superlattice and the structural details of the constituent molecules, the size of the cooperative unit could be higher than, equal to, or smaller than that of random composition. Thus the finding that the cooperativity versus compositions plots (Figure S6 in the Supporting Information) appears to display both maxima and minima coinciding with predicted critical compositions is not unexpected.

Not all predicted critical compositions were observed in each PC/PE mixture. For instance, the critical X_{PE} of 0.286 was observed only for the DMPC/DLPC mixture, while those at 0.25 and 0.33 were observed for several PC/PE mixtures (Table 2). There could be several reasons for this. First, the stability of the predicted superlattices may vary significantly, and thus those of lesser stability could remain unnoticed. The stability of a particular superlattice depends on the interactions between the component lipids, which could be highly sensitive to minor variations in structure. Notably, our previous analysis of calorimetric data published by others[25,26] showed that the effect of cholesterol on the transition enthalpy of phospholipids is highly sensitive to the acyl chain length, as shown by the fact that the number of perturbed acyl chains in the second layer proximal to cholesterol increases from 1 to 9 when the acyl chain length decreases from 20 to 14 carbons.[27] Also the previous calorimetric studies on PC/PE bilayers have shown that the phase behavior is highly sensitive to the acyl chain length of the components.[11,28]

The critical X_{PE}'s at 0.286, 0.40, and 0.600 are not predicted by the original SL model assuming the presence of monomeric quest only.[2,3,19] However, they can be explained by assuming the formation of a dimeric guest as shown in Figure S7C in the Supporting Information. The dimeric guest would be PE at X_{PE}'s of 0.286 and 0.40 and PC at X_{PE} of 0.60. The reasons for the presence of putative guest dimers are not obvious, but could relate to the intermolecular hydrogen bonding between PE molecules.[29] Such hydrogen bonding could stabilize dimeric PE guest directly and dimeric PC guest indirectly, i.e., formation of a hydrogen bonded network among PE hosts could promote dimerization of PC molecules. The indicated critical

dx.doi.org/10.1021/jp2078488 | J. Phys. Chem. B 2012, 116, 1802−1811

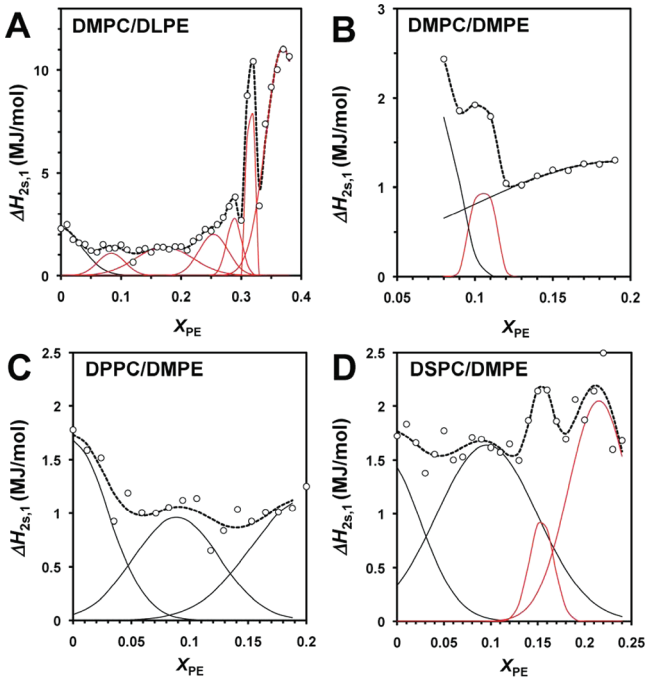

Figure 7. Two-state transition enthalpy of the pretransition ($\Delta H_{2S,1}$) versus X_{PE} for different PC/PE bilayers. See the caption of Figure 5 for details.

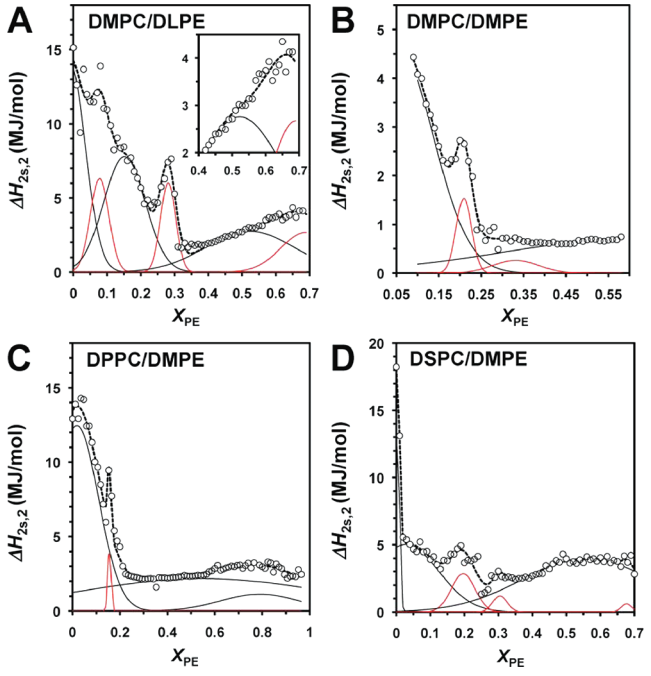

Figure 8. Two-state transition enthalpy for the first resolved component of the main transition ($\Delta H_{2S,2}$) versus X_{PE} for different PC/PE bilayers. (A) DMPC/DLPE, (B) DMPC/DMPE, (C) DPPC/DMPE, and (D) DSPC/DMPE. See the caption of Figure 5 for details.

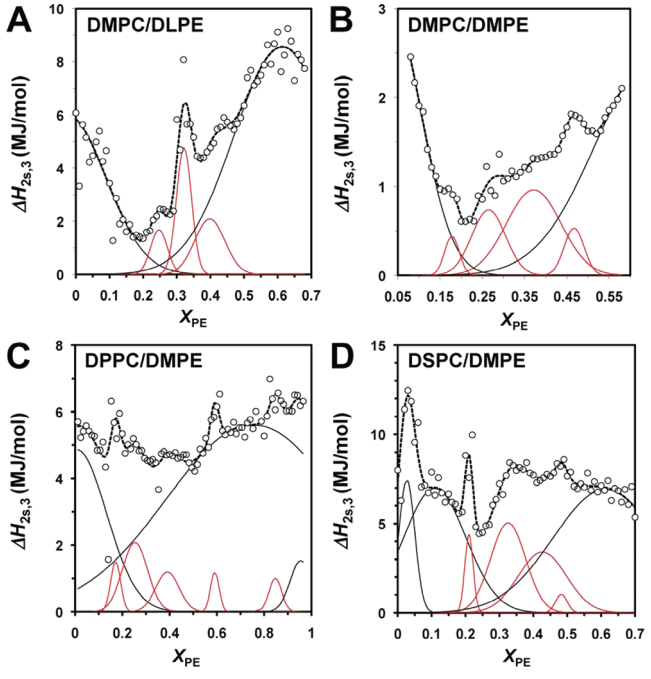

Figure 9. Two-state transition enthalpy for the second resolved component of the main transition ($\Delta H_{2S,3}$) versus X_{PE} for different PC/PE bilayers. (A) DMPC/DLPE, (B) DMPC/DMPE, (C) DPPC/DMPE, and (D) DSPC/DMPE. See the caption of Figure 5 for details.

composition at $X_{PE} \sim 0.546$ is neither predicted by the monomeric quest model nor attributable to the formation of guest dimers. We speculate that it might be due to the fusion of the enthalpic peaks deriving from superlattices with X_{PE} of 0.50 and 0.60.

In this study the total amount of phospholipid per sample was fixed at 1 μmol. We realize that this may result in missing some minor and/or very broad transitions. However, since we were primarily interested in identifying abrupt changes in the thermodynamic parameters over a narrow composition range, we opted to maintain a constant total lipid concentration. A more relevant concern is the composition of multilamellar liposomes, i.e., their true composition could deviate from the nominal one due to errors in pipetting the lipid mixtures. However, we have no reason to doubt that the actual compositions would differ more than ±1 mol % from the nominal ones because (1) extra care was taken when pipetting the samples using precision syringes (see Materials and Methods), (2) our previous tests[16] have shown that this accuracy can be achieved routinely, and (3) T_m versus composition plots do not show obvious signs of significant errors in composition (scatter). Another concern is that some liposome preparations could be inhomogeneous, i.e., consisting of population of different compositions. Since we did not detect any transitions due to pure PE or PC in the mixed samples, extensive segregation of the component lipids to different liposome populations is unlikely. However, it is not possible to fully exclude *partial* segregation. This issue might be resolved by carrying out extensive imaging and spectroscopic studies, but these are beyond the scope of this study. Nevertheless, we think that heterogeneity of the liposomes cannot explain our results, since extra care was taken to prevent component segregation when preparing the liposomes (see Materials and Methods). Most importantly, it is difficult to see how liposomal heterogeneity would result in multiple, abrupt changes in thermodynamic parameters and why these would occur at or close to the critical composition predicted by the SL model.

The formation of superlattices in PC/PE bilayers probably relates to the complementary shapes of PC and PE. The cross-sectional area of the highly hydrated headgroup of PC is larger than the cross-sectional area of its acyl chains,[30,31] which results

dx.doi.org/10.1021/jp2078488 | J. Phys. Chem. B 2012, 116, 1802–1811

in crowding at the headgroup level. Inclusion of PE, which has a much smaller headgroup, relieves such crowding when mixed with PC. This "spacer effect" is obviously maximal when PE is evenly distributed in the PC matrix and thus drives the formation of SL-like arrangements.[2]

The lack of significant hysteresis indicated by the similarity of the heating and cooling scans implies that the tendency to adopt SL-like lateral arrangements is maintained in the liquid-crystalline state as well. However, due to the diminished lateral packing in this state, the size and stability of superlattice domains are likely to significantly diminish. The existence of SL-like domains in liquid-crystalline PC/PE bilayers is supported by previous fluorescence and FTIR data.[7−9,32] Notably, while long-range order is unlikely to exist in the liquid-crystalline state, a high degree of *local* lateral order can exist, as found previously for the smectic A′ phase.[5]

We have previously proposed that superlattice formation could play a key role in the regulation of the composition of biological membranes.[2,3] While most of the data supporting this idea comes from studies on model membranes, it is intriguing that the phospholipid compositions of the erythrocyte and platelet membranes from several mammalian species coincide remarkably well with the critical compositions predicted by the superlattice model.[19] Since calorimetry mainly provides information on the gel state, it is not straightforward to project the present results on natural membranes, which are typically in the liquid-crystalline or liquid-order state. However, it seems feasible that the superlattice organization in the gel state is maintained above the phase transitions, i.e., in the liquid-crystalline state, albeit over a shorter length scale. Supporting this, spectroscopic studies on liquid-crystalline PE/PC bilayers have revealed similar critical compositions as in the present study.[7−10] It is also notable that some biological membranes or similar lipid assemblies could be in the gel (or similar) state at the physiological temperature. The best example is stratum corneum, the outermost layer of mammalian skin, in which the lipids are laterally highly ordered as shown by diffraction studies.[33] It seems likely that the lipids in stratum corneum adopt an SL-like lateral organization. It is also probable that rafts or similar liquid-order domains have a superlattice-like lateral organization of a short range.

5. CONCLUSIONS

In conclusion, this DSC study provides evidence that the molecules in binary PC/PE bilayers tend to adopt regular, SL-like lateral arrangements, which could be involved in the regulation of the lipid compositions of biological membranes.

■ ASSOCIATED CONTENT

Supporting Information

Additional information on the simulations of multiple two-state transition parameters and cooperativity (S1), the DSC scans of DMPC/DMPE (S2), the comparisons of heating, cooling and slow scans of DMPC/DLPE bilayers (S3), the χ^2 values versus composition plots (S4), the resolved thermodynamic parameters on DSPC/DEPE bilayers (S5), the estimation of the number of a cooperative unit in DMPC/DLPE bilayers (S6), the graphical comparison of predicted and observed critical compositions (S7), and the statistical analysis of the distribution of experimental versus predicted critical compositions using the binomial distribution model (S8). This information is available free of charge via the Internet at http://pubs.acs.org.

■ AUTHOR INFORMATION

Corresponding Author

*Address: Department of Physics and Astronomy, Trinity University, One Trinity Place, San Antonio, Texas 78212-7200, United States. E-mail: kcheng1@trinity.edu. Tel: 210-999-8469. Fax: 210-999-7421.

■ ACKNOWLEDGMENTS

This work was supported by a Robert A. Welch Research Foundation grant (D-1158), the Williams endowment fund of Trinity University, and an NIH grant (RC1-GM090897-02) given to K.H.C. and grants from the Finnish Academy and Sigrid Juselius Foundation to P.S.

■ REFERENCES

(1) Simons, K.; Gerl, M. J. *Nat. Rev. Mol. Cell Biol.* **2010**, *11*, 688−699.
(2) Somerharju, P.; Virtanen, J. A.; Cheng, K. H.; Hermansson, M. *Biochim. Biophys. Acta* **2009**, *1788*, 12−23.
(3) Somerharju, P.; Virtanen, J. A.; Cheng, K. H. *Biochim. Biophys. Acta* **1999**, *1440*, 32−48.
(4) Chong, P. L.; Zhu, W.; Venegas, B. *Biochim. Biophys. Acta* **2009**, *1788*, 2−11.
(5) Chou, C.-F.; Jin, A. J.; Hui, S. W.; Huang, C. C.; Ho, J. T. *Science* **1998**, *280*, 1424−1426.
(6) Hermansson, M.; Hokynar, K.; Somerharju, P. *Prog. Lipid Res.* **2011**, *50*, 240−257.
(7) Cheng, K. H.; Virtanen, J.; Somerharju, P. *Biophys. J.* **1999**, *77*, 3108−3119.
(8) Cheng, K. H.; Ruonala, M.; Virtanen, J.; Somerharju, P. *Biophys. J.* **1997**, *73*, 1967−1976.
(9) Cheng, K. H.; Cannon, B.; Metze, J.; Lewis, A.; Huang, J.; Vaughn, M. W.; Zhu, Q.; Somerharju, P.; Virtanen, J. *Biochemistry* **2006**, *45*, 10855−10864.
(10) Cannon, B.; Lewis, A.; Metze, J.; Thiagarajan, V.; Vaughn, M. W.; Somerharju, P.; Virtanen, J.; Huang, J.; Cheng, K. H. *J. Phys. Chem. B* **2006**, *110*, 6339−6350.
(11) Sugar, I.; Monticelli, G. *Biophys. Chem.* **1983**, *18*, 281−289.
(12) Silvius, J. R.; Brown, P. M.; O'Leary, T. J. *Biochemistry* **1986**, *25*, 4249−4258.
(13) Mabrey, S.; Sturtevant, J. M. *Proc. Natl. Acad. Sci. U.S.A.* **1976**, *73*, 3862−3866.
(14) Blume, A.; Wittebort, R. J.; Das Gupta, S. K.; Griffin, R. G. *Biochemistry* **1982**, *21*, 6243−6253.
(15) Blume, A.; Ackermann, T. *FEBS Lett.* **1974**, *43*, 71−74.
(16) Haimi, P.; Hermansson, M.; Batchu, K. C.; Virtanen, J. A.; Somerharju, P. *J. Biol. Chem.* **2010**, *285*, 751−760.
(17) Rubenstein, J. L. R.; Owicki, J. C.; McConnell, H. M. *Biochemistry* **1980**, *19*, 569−573.
(18) Cooper, A.; Nutley, M. A.; Wadood, A. *Protein−Ligand Interactions: Hydrodynamics and Calorimtery*; Harding, S. E., Chowdhry, B. Z., Eds.; Oxford University Press: New York, 2001; pp 289−318.
(19) Virtanen, J. A.; Cheng, K. H.; Somerharju, P. *Proc. Natl. Acad. Sci. U.S.A.* **1998**, *95*, 4964−4969.
(20) Small, D. M. *Handbook of Lipid Research*; Hanaham, D. K., Ed.; Plenum Press: New York, 1986; pp 97−143.
(21) Lentz, B. R.; Freire, E.; Biltonen, R. L. *Biochemistry* **1978**, *17*, 4475−4480.
(22) Black, S. G.; Dixon, G. S. *Biochemistry* **1981**, *20*, 6740−6744.
(23) Mendenhall, W.; Sincich, T. *Statistics for Engineering and the Sciences*; Dellen Publishing Co.: San Francisco, CA, 1992.
(24) Zhu, Q.; Cheng, K. H.; Vaughn, M. W. *J. Phys. Chem. B* **2007**, *111*, 11021−11031.
(25) McMullen, T. P. W; McElhaney, R. N. *Biochemistry* **1997**, *36*, 4979−4986.

(26) McMullen, T. P. W; Lewis, R. N. A. H.; McElhaney, R. N. *Biochemistry* **1993**, *32*, 516−522.
(27) Virtanen, J. A.; Somerharju, P. *J. Phys. Chem.* **1999**, *103*, 10289−10293.
(28) Sugar, I. P.; Monticelli, G. *Biophys. J.* **1985**, *48*, 283−288.
(29) Ghosh, R. *Biochemistry* **1988**, *27*, 7750−7758.
(30) McIntosh, T. J. *Biophys. J.* **1980**, *29*, 237−245.
(31) Israelachvili, J. N.; Mitchell, D. J. *Biophys. Biochim. Acta* **1975**, *389*, 13−19.
(32) Cannon, B.; Lewis, A.; Metze, J.; Thiagarajan, V.; Vaughn, M. W.; Somerharju, P.; Virtanen, J.; Huang, J.; Cheng, K. H. *J. Phys. Chem. B* **2006**, *110*, 6339−6350.
(33) Bouwstra, J. A.; Ponec, M. *Biochim. Biophys. Acta* **2006**, *1758*, 2080−2095.